

# Thermal Conductivity of the Rare-Earth Strontium Aluminates

Chunlei Wan,<sup>‡</sup> Taylor D. Sparks,<sup>§</sup> Pan Wei,<sup>‡</sup> and David R. Clarke<sup>†,¶</sup>

<sup>‡</sup>Materials Science and Engineering Department, Tsinghua University, Beijing 100084, China

<sup>§</sup>Materials Department, College of Engineering, University of California, Santa Barbara 93106

<sup>¶</sup>School of Engineering and Applied Sciences, Harvard University, Cambridge, Massachusetts 02138

The thermal conductivity of a series of complex aluminates,  $\text{RE}_2\text{SrAl}_2\text{O}_7$ , with different rare-earth (RE) ions, has been measured up to 1000°C. There is a strong dependence on the atomic number of the RE ion, ranging from an approximately  $1/T$  dependence for the lanthanum strontium aluminate to an almost temperature-independent behavior of the dysprosium strontium aluminate. The latter conductivity is comparable with that of yttria-stabilized zirconia, the current material of choice for thermal barrier coatings. The temperature dependence of the thermal conductivities of all the aluminates studied can be fit to a standard phonon–phonon scattering model, modified to account for a minimum phonon mean free path, in which the difference in behavior is attributed to increased phonon–phonon scattering with the atomic mass of the RE ion. Although a satisfactory parametric fit is obtained, the model does not take into account either the detailed layer structure of the aluminates, consisting of alternating rock-salt and perovskite layers in a natural superlattice structure, or the site preferences of the RE ion. This suggests that further model development is warranted.

## I. Introduction

THE majority of data in the literature on the thermal conductivity of oxides have been obtained on oxides with relatively simple crystal structures and compositions.<sup>1</sup> In seeking alternatives for low thermal conductivity applications at high temperatures, there has been growing interest in more complicated compositions and more complex crystal structures. There is also increasing interest in identifying compounds that exhibit anisotropic thermal conductivity for different applications. A number of oxides are crystallographically anisotropic, such as the Ruddlesden–Popper<sup>2,3</sup> and Aurivillius<sup>4</sup> phases. The majority of these compounds are based on perovskite-like blocks consisting of  $\text{TiO}_6$  octahedra. While the titanate-based structures are the most well known, there are also layered and crystallographically anisotropic compounds based on aluminate-based perovskite structures. Of these, the rare-earth (RE) strontium aluminates,<sup>5</sup> with the formula  $\text{RE}_2\text{SrAl}_2\text{O}_7$ , are particularly interesting. They are the structural counterparts of the RE manganites, which have generated interest on account of their magnetic and electronic properties. An unusual feature of the crystal structure of the RE strontium aluminates is that it can be thought of as consisting of a stacking of double-perovskite blocks, formed by  $\text{AlO}_6$  octahedra, alternating with a rocksalt block, Figure 1. The  $\text{Sr}^{2+}$  and  $\text{RE}^{3+}$  ions are distributed between two sites: one in the rocksalt block and the other in the perovskite block.

D. J. Green—contributing editor

Manuscript No. 26353. Received June 11, 2009; approved December 9, 2009.  
This work was supported by National Science Foundation's Materials World Network grant DMR-0710523 and the China National Science Foundation.

<sup>†</sup>Author to whom correspondence should be addressed. e-mail: clarke@seas.harvard.edu

In this contribution, we present the results of an exploratory investigation of the thermal conductivity of this unusual class of oxides in which the RE ion was systematically varied from La, ..., Dy. Considerable structural information about these complex aluminates, including lattice parameters, unit cell volume, interatomic distances, and cation ordering, has been reported.<sup>5</sup> As will be shown, although there is little difference in the ionic size and mass of the RE ions in the compounds investigated, there are dramatic differences in their thermal conductivity.

## II. Experimental Procedure

Following the method described by Zvereva *et al.*,<sup>5</sup> four of the aluminates, with RE = Sm, Eu, Gd, and Dy, were prepared from stoichiometric mixtures of the oxides with  $\text{SrCO}_3$  powders, which were calcined at 1100°C for 8 h, ground, and then sintered at 1550°C for 5 h in air. Before mixing, the RE oxides were heated for 8 h at 1000°C to remove any adsorbed  $\text{CO}_2$  and  $\text{H}_2\text{O}$ . The other two aluminates,  $\text{La}_2\text{SrAl}_2\text{O}_7$  and  $\text{Nd}_2\text{SrAl}_2\text{O}_7$ , could not be made phase pure by mixing oxides. Instead, they were prepared using a coprecipitation method from nitrate solutions. The mixed nitrate solutions were slowly added to ammonia to produce gel-like precipitates that were washed and filtered and then washed in ethyl alcohol. The washed precipitates were dried overnight at 120°C and then calcined at 900°C for 5 h before grinding, cold pressing, and sintering in air at 1550°C for 5 h. The densities were measured using the Archimedes method. Elastic constant measurements were performed by sonic velocity measurements. Powders were characterized by X-ray diffraction and their specific heat was measured as a function of temperature using a Netzsch Pergasus DSC system (Selb, Bavaria, Germany).

The thermal diffusivity of each of the aluminates was measured as a function of temperature up to 1000°C using the thermal flash technique. The measurements were made on disk-shaped samples whose sides were first coated with a very thin adhesion layer of Ti, followed by a 100 nm layer of Pt. These coatings were used to minimize the possibility of any pin holes through which the light flash could propagate through the samples to the detector. The samples were then spray coated with a thin layer of carbon on both sides. The measurements were made using an Anter 3000 Flashline system (Pittsburgh, PA) with a Xenon flash lamp as the heat source.

## III. Results

All six of the aluminate compounds synthesized were phase pure as assessed by X-ray diffraction and exhibited the peak height distributions expected for a random, polycrystalline material. Observations of polished sections using the electron back-scattered mode of the SEM revealed that each of the samples contained less than about 3% of any second phase as a discrete second phase. With the exception of the  $\text{La}_2\text{SrAl}_2\text{O}_7$  compound,

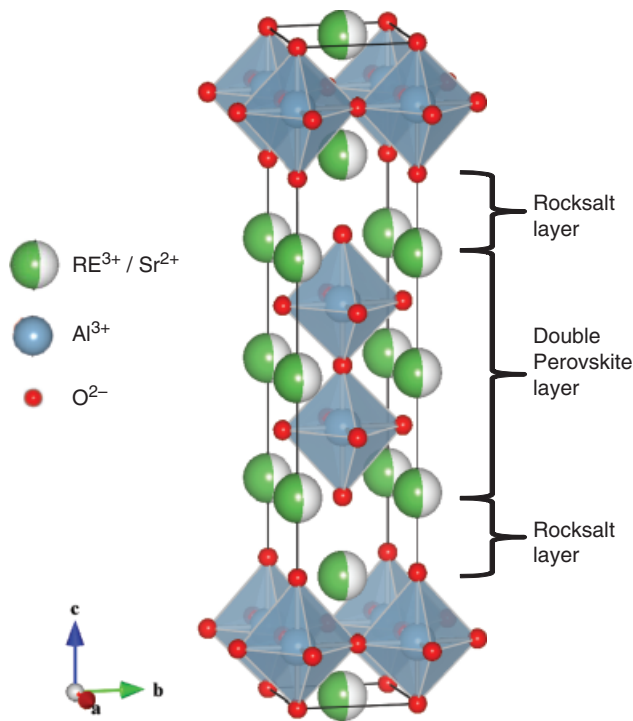


**Fig. 1.** Crystal structure of the rare-earth strontium aluminates. The structure consists of a double perovskite layer, formed of  $\text{AlO}_6$  octahedra, separated by a layer of rock-salt stacking. Drawn using VESTA software.<sup>20</sup>

the densities were all  $>95\%$  of their theoretical values (Table I). In contrast to the other compositions, this material consisted of long lamellae grains with small pores at the intercept of the lamellae grains. Also listed in Table I are the Young's modulus of the materials. The specific heats of the individual aluminates are plotted in Fig. 2, and the measured thermal diffusivities are plotted in Fig. 3.

The thermal conductivities were calculated from the measured diffusivities,  $\alpha$ , densities,  $\rho$ , and specific heat values,  $C_p$ , using the standard relationship:

$$k = \rho C_p \alpha \quad (1)$$

The values of conductivity determined in this way are plotted in Fig. 4.

#### IV. Discussion

Two striking features of the thermal conductivity data are shown in Fig. 4. The first is the remarkable difference in the thermal conductivity with temperature of the different RE strontium aluminates. Furthermore, because the difference in the ionic size and ionic mass between the RE ions in the aluminates studied is relatively small, it is surprising that this can account for the observed temperature dependence. The second is the

**Table I. Physical Properties**

Composition	X-ray density (kg/m <sup>3</sup> )	Relative density	Young's modulus (GPa)	Unit cell volume (nm <sup>3</sup> )
$\text{La}_2\text{SrAl}_2\text{O}_7$	5.711	0.881	166.4	0.2872
$\text{Nd}_2\text{SrAl}_2\text{O}_7$	5.914	0.990	186.0	0.2783
$\text{Sm}_2\text{SrAl}_2\text{O}_7$	6.082	0.948	252.3	0.2744
$\text{Eu}_2\text{SrAl}_2\text{O}_7$	6.193	0.980	240.0	0.2730
$\text{Gd}_2\text{SrAl}_2\text{O}_7$	6.343	0.955	257.9	0.2716
$\text{Dy}_2\text{SrAl}_2\text{O}_7$	6.508	0.962	230.4	0.2686

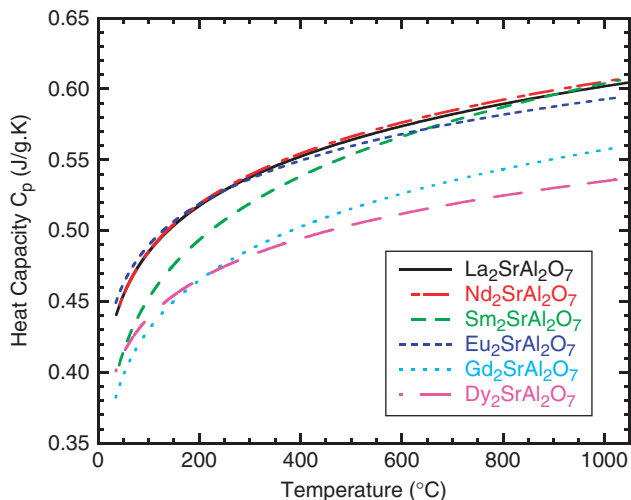


**Fig. 2.** Specific heat as a function of temperature of the individual aluminates.

unusually low thermal conductivity of all the aluminates in approaching the high-temperature limit, where the conductivity is independent of temperature.

To place the conductivities in context, the thermal conductivities are intermediate between those of simple defect-free oxides, such as aluminum oxide, MgO, and monoclinic zirconia,<sup>1,6</sup> and defective crystals such as yttria-stabilized zirconia.<sup>1,6-8</sup> From comparison of their temperature dependence, the behavior of the lanthanum strontium aluminate is similar to that of monoclinic zirconia, whereas that of the dysprosium strontium aluminate is similar in nature to that of yttria-stabilized zirconia. The other aluminates lie between these two contrasting behaviors. The comparisons are revealing because the marked temperature dependence of monoclinic zirconia is characteristic of the  $\sim 1/T$  dependence attributed to anharmonic phonon scattering observed in oxides that do not contain high concentrations of point defects or other scattering centers. Similar behavior is also reported for the majority of oxides. In contrast, the temperature independence of yttria-stabilized zirconia is characteristic of oxides containing such a high concentration of scattering defects that the mean phonon scattering length is of interatomic dimensions at room temperature or thereabouts.<sup>6,9-11</sup> In the case of yttria-stabilized zirconia, the point defects are oxygen vacancies introduced to charge compensate for the alio-valent stabilizing yttrium ion ( $\text{Y}^{3+}$ ). None of the

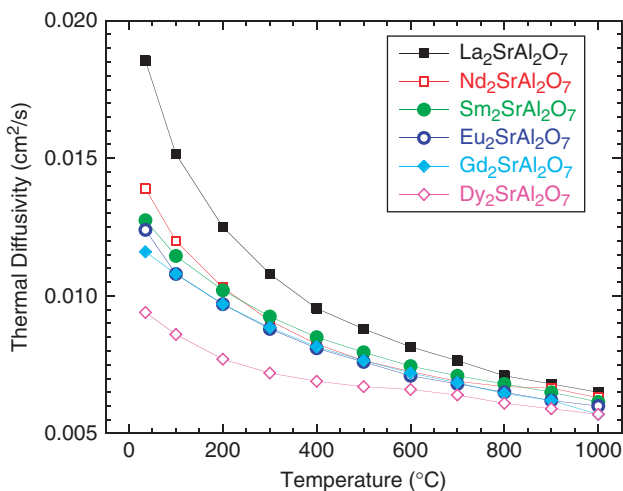


**Fig. 3.** Thermal diffusivity as a function of temperature of the aluminates measured by the thermal flash technique.

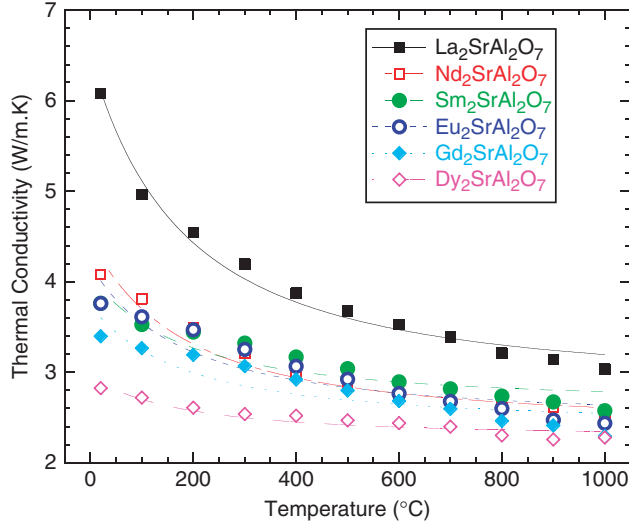


**Fig. 4.** Thermal conductivity of the aluminates as a function of temperature. The lines through the data points represent the fits to Eq. (8) in the text and with the fitting parameters listed in Table II.

RE strontium aluminates contains oxygen vacancies or any other structural defects, and so the contrasting behavior of the different aluminates is likely to have a different origin.

The lattice thermal conductivity of pure, electrically insulating, defect-free crystalline solids has been studied theoretically in considerable detail.<sup>12–15</sup> From models for anharmonic phonon scattering, the thermal conductivity as a function of temperature at high temperatures can be written in the form:

$$k = \frac{A}{T} \quad (2)$$

where the parameter  $A$  can be expressed in terms of atomistic and crystal structure properties:

$$A = \frac{B'}{(2\pi)^3} \bar{M} \bar{\Omega}^{1/3} \frac{k_B^3 \Theta_D^3}{h^3 \gamma^2} \quad (3)$$

$\bar{M}$  is the average atomic mass of the atoms in the unit cell,  $\bar{\Omega}$  is the average atomic volume (the volume of the unit cell divided by the number of atoms in the unit cell),  $\gamma$  is the Gruneisen constant, and  $B'$  is a constant. It has been suggested that the value of the constant  $B'$  is approximately unity, 1.61, according to Klemens,<sup>13</sup> but according to Leibfried and Schlomann after correction for a numerical error,<sup>16</sup> it is 10.9. The other constants are the Boltzmann and Planck's constants and  $\Theta_D$  is the Debye temperature. In turn, the Debye temperature can be expressed in terms of the acoustic velocity,  $v$ , and the mean atomic size,  $\Omega^{1/3}$

$$\Theta_D = \frac{vh}{k_B} \left( \frac{3\pi^2}{\Omega} \right)^{1/3} \quad (4)$$

If the acoustic velocity is taken to be the mean wave velocity,  $v_m$

$$v_m = 3^{1/3} \left( \frac{1}{\rho_p^3} + \frac{2}{\rho_s^3} \right)^{-1/3} \quad (5)$$

Then to a very good approximation, this can be written in terms of the Young's modulus,  $E$ , and the density, expressed in terms of the mean atomic mass and the mean atomic volume:<sup>17</sup>

$$v_m = 0.87 \sqrt{\frac{E}{\rho}} = 0.87 \sqrt{\frac{E\bar{\Omega}}{M}} \quad (6)$$

Taken together, the thermal conductivity can be written as

$$K = \frac{E^{3/2} \bar{\Omega}^{5/6}}{2\pi\gamma^2 \bar{M}^{1/2}} \frac{B'}{T} \quad (7)$$

At high temperatures, above the Debye temperature, the phonon frequency distribution increases with temperature and the mean free path approaches the minimum possible in a crystalline solid, namely the interatomic spacing. This modifies the temperature dependence of the anharmonic phonon scattering from the  $1/T$  dependence expressed in Eqs. (2) and (7). To account for the minimum phonon mean free path, Mevrel *et al.*<sup>18</sup> have suggested that the thermal conductivity can then be written in the form:

$$k = \frac{A}{T} \left[ \frac{2}{3} \sqrt{\frac{T_1}{T}} + \frac{T}{3T_1} \right] = \frac{2A\sqrt{T_1}}{3T^{3/2}} + \frac{A}{3T_1} \quad (8)$$

where the second term,  $\frac{A}{3T_1}$ , is the limiting value of the thermal conductivity at high temperatures, also referred to as  $k_{\min}$ , when the phonon mean free path is the same as the mean interatomic spacing. In contrast to Eqs. (2) and (7), this equation predicts a more complex temperature dependence, as observed, than the simple  $1/T$  dependence in conventional models.

In comparing our experimental data with Eq. (8), the parameters  $A$  and  $T_1$  can be used as fitting parameters. The best regression fits to the data for the thermal conductivity of the aluminates are shown by the lines through the data in Fig. 4 and the values for the fitting parameters are listed in Table II. The  $R^2$  values are reasonable, given the relatively small number of data points, indicating a good fit to the conductivity data, except for the Gd aluminate data. The form of the Eq. (7) suggests that there is a  $\bar{M}^{-1/2}$  mass dependence for the parameter  $A$ , which is, as shown in Fig. 5, indeed consistent with our results.

As evidenced by the quality of the fits to the data for the different RE aluminates, the anharmonic phonon scattering model, including the phonon wavelength cut-off proposed by Mevrel *et al.*,<sup>18</sup> represents both the temperature and the mass dependence of the thermal conductivity of these compounds. However, it should be emphasized that while the rank ordering of the aluminates is captured through the value of the parameter  $A$ , the model does not predict the value of  $A$  or the absolute values of the thermal conductivity.

Although the finding that the temperature dependence of the thermal conductivity of the series of RE strontium aluminates is consistent with existing models of anharmonic phonon scattering, it is rather unsatisfactory as the models assume that the material is homogeneous and isotropic and yet the crystal structure is a crystallographically highly anisotropic natural superlattice structure consisting of alternating layers of perovskite and rock-salt blocks as shown in Fig. 1. At very high temperatures, where the phonon scattering length approaches the spacing between atoms, it is reasonable to expect that the detailed atomic arrangement may not affect the phonon scattering, but

**Table II.** The Fitting Parameters for the RE<sub>2</sub>SrAl<sub>2</sub>O<sub>7</sub> (RE = La, Nd, Sm, Eu, Gd, Dy) series

Rare-earth Ion	La	Nd	Sm	Eu	Gd	Dy
$A$ (W/m)	1730	1153	934	998	725	525
$T_1$ (K)	207	167	118	135	100	77
$R^2$	0.984	0.962	0.851	0.862	0.648	0.898
$K_{\min}$ (W/mK)	2.77	2.31	2.64	2.47	2.42	2.27

RE, rare earth.

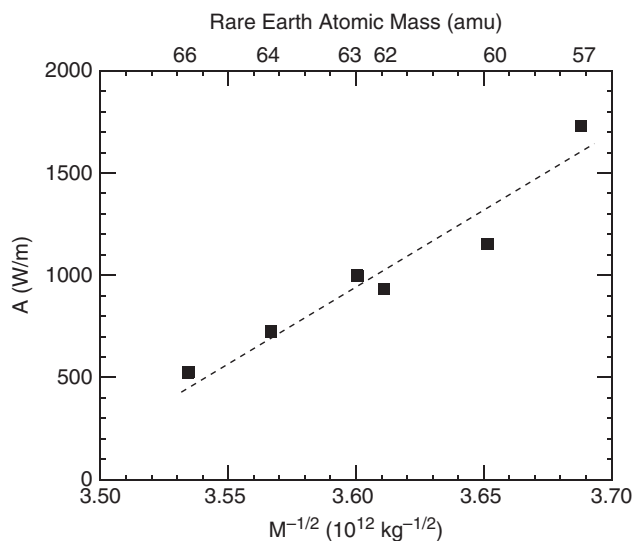


**Fig. 5.** Demonstration that the fitting parameter,  $A$ , varies as the inverse square root of the mean atomic mass,  $M$ , of the individual aluminates. The top scale represents the atomic mass of the rare-earth ion.

over the temperature range we have investigated, the phonon mean free paths are larger than this minimum value and so one would expect that the phonon scattering would be sensitive to the layered structure of the compounds. The other feature of these aluminates not incorporated within the phonon scattering model is that the distribution of the RE ions within the rock-salt and perovskite blocks varies with the atomic number; specifically, there is an increasing site preference of the RE ion for the rock-salt block with increasing atomic number of the RE from  $\text{La}^{3+}$  to  $\text{Dy}^{3+}$ . This results in the relative densities of the two blocks changing with increasing atomic number.<sup>19</sup> It is, therefore, tempting to believe that the thermal conductivity and its temperature dependence are determined by a combination of interblock mass scattering and standard anharmonic phonon scattering. However, no phonon scattering model that we are aware of currently takes into account these detailed crystallographic features or the layered structure of the unit cell of materials such as these aluminates, suggesting that more refined models are necessary to describe complex, layered structures.

## V. Conclusions

The thermal conductivity of the RE strontium aluminates up to 1000°C is found to be strongly dependent on the individual RE ion even though the REs that can form the complex strontium-aluminate structure can only vary over a very narrow range of atomic weight, from  $\text{La}^{3+}$  (138.9 amu) to  $\text{Ho}^{3+}$  (164.9 amu). The temperature dependence of all the compounds can be well

represented by the standard anharmonic phonon scattering model modified to account for a minimum phonon mean free path. The lowest thermal conductivity of the series of compounds, that of the dysprosium strontium aluminate, is comparable with that of yttria-stabilized zirconia despite the fact that the aluminates do not contain oxygen vacancies as the zirconia does.

## Acknowledgment

The authors are grateful to colleagues in the NSF's Materials World Network, notably Professor Simon Phillpot, University of Florida, for helpful discussions.

## References

- W. D. Kingery, "Thermal Conductivity: XII, Temperature Dependence of Conductivity for Single-Phase Ceramics," *J. Am. Ceram. Soc.*, **38** [7] 251–5 (1955).
- S. N. Ruddlesden and P. Popper, "New Compounds of the  $\text{K}_2\text{NiF}_4$  Type," *Acta Crystallogr.*, **10**, 538–9 (1957).
- S. N. Ruddlesden and P. Popper, "The Compound  $\text{Sr}_3\text{Ti}_2\text{O}_7$  and Its Structure," *Acta Crystallogr.*, **11**, 54–5 (1958).
- B. Aurivillius, "Mixed Bismuth Oxides with Layer Lattices. II. Structure of  $\text{Bi}_4\text{Ti}_3\text{O}_{12}$ ," *Arkiv für Kemi*, **1**, 499–512 (1949).
- I. Zvereva, Y. Smimov, V. Gusarov, V. Popova, and J. Choisnet, "Complex Aluminates  $\text{RE}_2\text{SrAl}_2\text{O}_7$  (RE = La, Nd, Sm-Ho): Cation Ordering and Stability of the Double Perovskite Slab-Rocksalt Layer P-2/RS Intergrowth," *Solid State Sci.*, **5** [2] 343–9 (2003).
- D. R. Clarke and S. R. Phillpot, "Thermal Barrier Coating Materials," *Mater. Today*, **8** [6] 22–9 (2005).
- J. F. Bisson, D. Fournier, M. Poulain, O. Lavigne, and R. Mevrel, "Thermal Conductivity of Yttria-Zirconia Single Crystals, Determined with Spatially Resolved Infrared Thermography," *J. Am. Ceram. Soc.*, **83** [8] 1993–8 (2000).
- R. Mevrel, J.-C. Laizet, A. Azzopardi, B. Leclercq, M. Poulain, O. Lavigne, and D. Demange, "Thermal Diffusivity and Conductivity of  $\text{Zr}_{1-x}\text{Y}_x\text{O}_{2-x/2}$  ( $x = 0, 0.084$  and  $0.179$ ) Single Crystals," *J. Eur. Ceram. Soc.*, **24** [10–11] 3081–9 (2004).
- M. R. Winter and D. R. Clarke, "Oxide Materials with Low Thermal Conductivity," *J. Am. Ceram. Soc.*, **90** [2] 533–40 (2007).
- P. G. Klemens, "Thermal Resistance Due to Point Defects at High Temperatures," *Phys. Rev.*, **119** [2] 507–9 (1960).
- P. G. Klemens, "Phonon Scattering by Oxygen Vacancies in Ceramics," *Phys. B*, **263–264**, 102–4 (1999).
- G. Grimvall, *Thermophysical Properties of Materials*, North Holland, Amsterdam, the Netherlands, 1986.
- P. G. Klemens, "Thermal Conductivity and Lattice Vibrational Modes," *Solid State Phys.—Adv. Res. Appl.*, **7**, 1–98 (1958).
- P. Carruthers, "Theory of Thermal Conductivity of Solids at Low Temperatures," *Rev. Modern Phys.*, **33** [1] 92–138 (1961).
- J. Callaway, "Model for Lattice Thermal Conductivity at Low Temperatures," *Phys. Rev.*, **113** [4] 1046–51 (1959).
- C. L. Julian, "Theory of Heat Conduction in Rare-Gas Crystals," *Phys. Rev.*, **137**, A128–37 (1965).
- D. R. Clarke, "Materials selection guidelines for low thermal conductivity thermal barrier coatings," *Surf. Coat. Technol.*, **163**, 67–74 (2003).
- R. Mevrel, J.-C. Laizet, A. Azzopardi, B. Leclercq, M. Poulain, O. Lavigne, and D. Demange, "Thermal Diffusivity and Conductivity of  $\text{Zr}_{1-x}\text{Y}_x\text{O}_{2-x/2}$  ( $x = 0, 0.084$  and  $0.179$ ) Single Crystals," *J. Eur. Ceram. Soc.*, **24** [10–11] 3081–9 (2004).
- T. D. Sparks, "Thermal Conductivity of Layered Oxides"; MS Thesis, University of California, Santa Barbara, 2010.
- K. Momma and F. Izumi, "VESTA: A Three Dimensional Visualization System for Electronic and Structural Analysis," *J. Appl. Crystallogr.*, **41**, 653–8 (2008). □